Comparing Fast Numerical Methods and Conventional CFD for Mixing Ventilation Flows

Eugene Mamulova [a], *Twan* van Hooff [a]

[a] Eindhoven University of Technology, Eindhoven, the Netherlands, e.mamulova@tue.nl.

Abstract. Computational fluid dynamics (CFD) provides detailed information on the flow inside a room and can thus be used for detailed analyses of the influence of design variables, such as the placement of ventilation openings. As a result, CFD is well-suited to the optimization of ventilation at room level. However, the high computational cost and level of expertise required for implementation constitute bottlenecks in the engineering sector. In this research, a number of fast numerical techniques such as voxel-based CFD (vCFD) and coarse grid CFD (cCFD) are implemented as alternatives to conventional CFD. The methods are used to predict the velocity field for a generic mixing ventilation case and their accuracy and speed are compared. Reynolds-averaged Navier-Stokes simulations using RNG $k-\epsilon$ closure are performed, using ANSYS Fluent, in series and in parallel. The vCFD simulation is executed using the commercially available software ANSYS Discovery 2021 R2, which utilizes a proprietary algorithm that runs on GPU. The results show that, for the isothermal case, the fast numerical methods (FNMs) are two orders of magnitude faster than CFD. The accuracy of vCFD, cCFD and CFD is very similar: All cases yield RMSE and FAC1.3 values in a similar range. Current results show that vCFD and cCFD offer accelerated performance when compared to CFD, while maintaining similar accuracy. FNMs offer a distinct advantage over engineering tools, in the form of spatial information, which decreases the uncertainty of local comfort calculations prescribed by building standards. Ongoing thermal simulations for, among other things, a displacement ventilation case, using CFD, vCFD and cCFD are expected to offer additional insight into the feasibility of FNMs in the context of ventilation design optimization.

Keywords. fast numerical methods, ventilation design, coarse-grid CFD, voxel-based modeling, computational fluid dynamics.
DOI: https://doi.org/10.34641/clima.2022.303

1. Introduction

Building ventilation quality has a large impact on the comfort, health and performance of building occupants [1]. Thus, the act of optimizing a ventilation design is of paramount importance to the engineer. Optimization criteria at room level include variables such as opening location and the shape of the supply openings [2,3]. There are three common approaches that may be employed in the act and they are outlined in **Fig. 1**. Engineering tools, computational fluid dynamics (CFD) and fast numerical methods (FNMs) each possess a characteristic trade-off between accuracy, computational cost and level of numerical expertise required for implementation.

The use of CFD for simulating indoor flows was pioneered by Nielsen in the 1970s [4]. CFD is capable of providing high-quality information on momentum, energy and mass transfer within a room. CFD methods range from transient large eddy simulations to steady-state Reynolds-averaged Navier-Stokes (RANS) simulations, the latter of which consume less resources. Nevertheless, steady RANS remains very costly, impeding its adoption in day-to-day design practices [5].

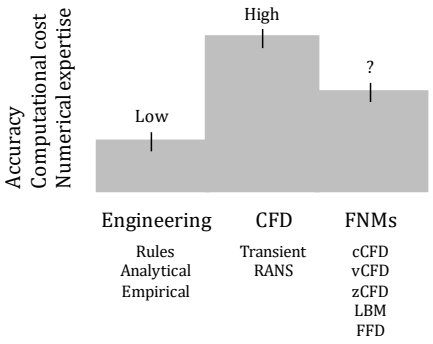

Fig. 1 – Qualitative accuracy-cost-expertise trade-off for engineering tools, CFD and FNMs.

Common engineering tools include rules of thumb, as well as analytical and empirical models that allow ventilation designers to make quick decisions and perform the calculations necessary for compliance with building quality standards. In contrast to CFD, engineering tools are very easy to apply and do not require any computational resources. However, the accuracy of the aforementioned methods is lower, as is the resultant spatial information.

Fast numerical methods constitute a compromise between the aforementioned approaches, such that they may potentially yield accuracies higher than engineering tools and most likely lower than CFD, while demanding less computational resources and modelling expertise than the latter [5]. Past studies encompass a vast variety of fast numerical methods, some of which are well-suited for indoor applications [6]. Fast numerical methods of interest include coarse-grid CFD (cCFD) [7], voxel-based CFD (vCFD) [8], zero-equation turbulence modeling (zCFD) [9], Lattice Boltzmann methods (LBM) [10] and fast fluid dynamics (FFD) [11]. The focus of this paper is on the application of cCFD and vCFD, which are both based on conventional CFD. cCFD makes use of a sub-optimal grid, yielding a solution that cannot be considered grid-independent. The reduced number of cells decreases the computation time, at the expense of accuracy. vCFD uses a voxel-based, Cartesian grid that is automatically generated [12]. The GPU-based implementation is expected to significantly speed up the computation.

The inclusion of FNMs in current ventilation design methodologies could potentially improve the quality of the design outcome. However, a comparative assessment of conventional CFD, fast numerical methods and empirical approaches is not yet available in literature, hindering the prospective development of an effective workflow for ventilation design. Moreover, the potential of fast numerical methods in terms of ensuring ventilation design quality has not yet been quantified. The main objective of this research is to test the speed and accuracy of vCFD, cCFD and CFD for an isothermal mixing ventilation case. This study compares the performance of empirical models, fast numerical methods and conventional CFD, in the aim to discuss whether the implementation of fast numerical methods in current engineering practice can improve ventilation design quality, as it is prescribed by current building standards.

2. Isothermal validation study

The isothermal case is based on measurement data collected by Nielsen [13]. The case involves a three dimensional enclosure with one inlet and one outlet. The measurements are performed for Re = 5000 and a kinematic viscosity v of 15.3 $\times 10^{-6}$m^2/s, at an air temperature of 20°C. The setup captures the flow penetration and recirculation that is characteristic of mixing ventilation, which makes it well-suited for the validation of mixing flow simulations. The geometry modeled in ANSYS Design Modeler is shown in **Fig. 2**. The length L, width W and height H are equal to 9 m, 3 m and 3 m, respectively. The inlet height h is equal to 0.168 m. The outlet height t is equal to 0.480 m. Inlet and outlet length l is equal to 3 m.

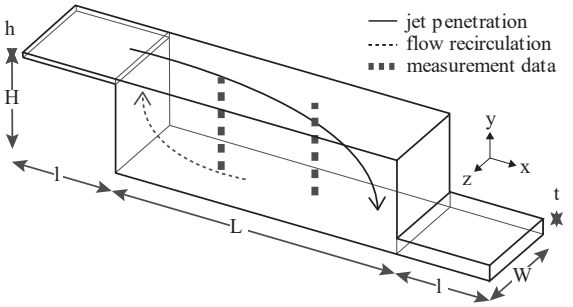

Fig. 2 – Room geometry including two measurement locations at z = 0.5W.

Validation data consists of 25 measurement points at x = H and 25 measurement points at x = 2H. The data is used to test the accuracy of the numerical methods. The validation metrics used, i.e. root-mean square error (RMSE) and factor of 1.1 of observations (FAC1.1) are defined in equations (1) and (2), where y_{CFD} and y_{EXP} represent simulated and measured values, respectively. In addition to FAC1.1, FAC1.2 and FAC1.3 are calculated. The equations are not shown for the sake of brevity.

$$\mathrm{RMSE} = \sqrt{\left(\sum_{n=1}^{N} \frac{(y_{CFD}-y_{EXP})^2}{N}\right)} \quad (1)$$

$$\mathrm{FAC1.1} = \frac{1}{N}\sum_{n=i}^{N} n_i,\ \ n_i = \begin{cases} 1\ for\ 0.91 \le \frac{y_{CFD_i}}{y_{EXP_i}} \le 1.1 \\ 0\ else \end{cases} \quad (2)$$

2.1 CFD methodology

The domain is discretized into hexahedral cells using ANSYS Meshing, as shown in **Fig. 3a**. A grid-sensitivity analysis is performed in order to establish a grid resolution that provides a nearly grid-independent solution. **Tab. 1** summarizes the key characteristics of the grids. Coarse is the coarsest possible grid to satisfy the requirement $y^* < 5$ for low Reynolds number modeling.

Tab. 1 – Summary of the computational grids.

Grid	Cell count	$y*_{max}$	$\overline{y^*}$
Coarse	265,650	6	4
Basic	766,250	4	3
Fine	2,211,863	3	2

The inlet velocity, $U_o = 0.455 m/s$, is obtained using the relation $Re = hU_o/v$. The static gauge pressure at the outlet is 0 Pa. The boundary conditions at the walls are no-slip. The turbulent kinetic energy k_0 and turbulent dissipation rate ϵ_o are scaled according to the inlet and outlet heights, using equations (3) and (4), where the turbulent length scale l_0 is taken to be 10% of the opening height and C_μ is a model constant, equal to 0.09.

$$k_0 = 1.5(0.04 \cdot U_0)^2 \quad (3)$$

$$\epsilon_0 = \frac{k_0^{1.5}}{l_0} \quad (4)$$

The resultant k_0 and ϵ_0 at the inlet are set to $5.0 \times 10^{-4}\ m^2/s^2$ and $6.6 \times 10^{-4}\ m^2/s^3$. Similarly, backflow k_0 and ϵ_0 are equal to $5.0 \times 10^{-4}\ m^2/s^2$ and $2.3 \times 10^{-4}\ m^2/s^3$, respectively.

The simulations are performed using the steady solver in ANSYS Fluent 2021 R1. The RANS equations are closed via the RNG $k-\epsilon$ model and low Reynolds number modeling is used for near-wall treatment. The settings are based on a comparison of experimental results with the results obtained using a range of RANS turbulence models, which is omitted for the sake of brevity. Pressure and velocity are coupled using the SIMPLE algorithm and the former is interpolated via the second order discretization scheme. The remaining terms are computed using the second order upwind scheme. Steady statistics are enabled after 1000 iterations and the sampling interval is set to 1. The under-relaxation factors for momentum, pressure, density, body forces, turbulent kinetic energy, turbulent dissipation rate and turbulent viscosity are set to 0.3, 0.6, 0.6, 0.3, 0.5, 0.5 and 0.6, respectively.

Due to oscillations in the residual values, the mean x-velocity component U_x is monitored at several points in the domain. The percentage deviation D between two iterations, 1000 iterations apart, is calculated and convergence is assumed when $D \leq 0.1$ %. Absolute convergence criteria for momentum, velocity and turbulence terms are not defined but all residual terms level off and drop by at least three orders of magnitude before the aforementioned convergence criteria for U_x are satisfied. The simulations are stopped after 35,000 iterations.

The grid-sensitivity analysis focuses on the dimensionless x-velocity profiles at $x = H$ and $x = 2H$, as shown in **Fig. 4**. The grid convergence index (GCI) is calculated using equation (5), where r is the linear grid refinement factor, equal to 2, p is the formal order of accuracy, equal to 2, and F_s is the safety factor, which takes the value 1.25 for a sensitivity analysis involving three or more grids.

$$GCI_{basic} = F_s \frac{r^p[(U_{basic} - U_{fine})/U_0]}{1 - r^p} \quad (5)$$

The results show that the coarse grid provides almost grid-independent results. The coarse grid is shown in **Fig. 3a**. The maximum and average GCI_{coarse} values at $x = H$ are 0.02 and 0.07 and the maximum and average GCI_{coarse} values at $x = 2H$ are 0.01 and 0.07, respectively.

2.2 cCFD methodology

The boundary conditions used for cCFD are identical to those used for CFD. The cCFD simulations are also performed using the steady solver in ANSYS Fluent 2021 R1. The RANS equations are closed via the RNG $k-\epsilon$ model and wall functions are used for near-wall treatment. Pressure and velocity are coupled using the Coupled scheme and the former is interpolated via the second order discretization scheme. The remaining terms are computed using the second order upwind scheme. Steady statistics are enabled after 1000 iterations and the sampling interval is set to 1. The under-relaxation factors for momentum, pressure, density, body forces, turbulent kinetic energy, turbulent dissipation rate and turbulent viscosity are set to default values of 0.5, 0.5, 1, 1, 0.8, 0.8 and 1, respectively. Convergence is assumed when all residual terms level off and drop by at least three orders of magnitude. The simulations are stopped after 1,500 iterations.

The meshing procedure consists of coarsening the CFD mesh while maintaining a smaller cell size closer to the wall and ensuring the presence of distinct cells at validation points $x = H$ and $x = 2H$. The cell count decreases from 265,650 cells for CFD to 4,401 cells for cCFD. The y^* values at the ceiling range from 5 to 12. The cCFD grid is shown in **Fig. 3b**.

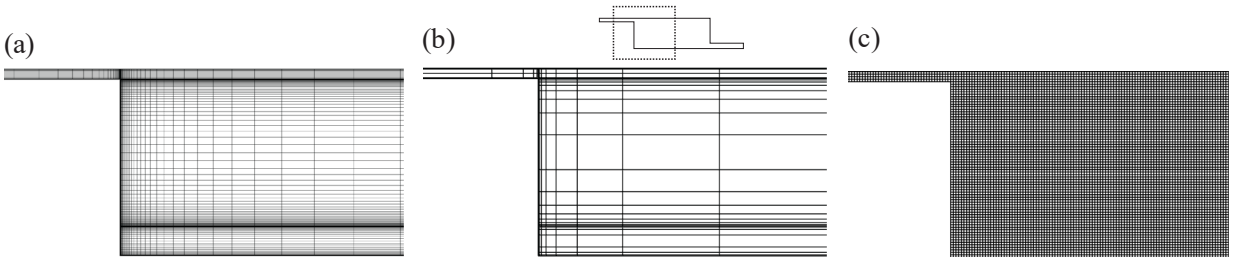

Fig. 3 – Two-dimensional, close-up view of the computational grids: (a) CFD, (b) cCFD, and, (c) vCFD.

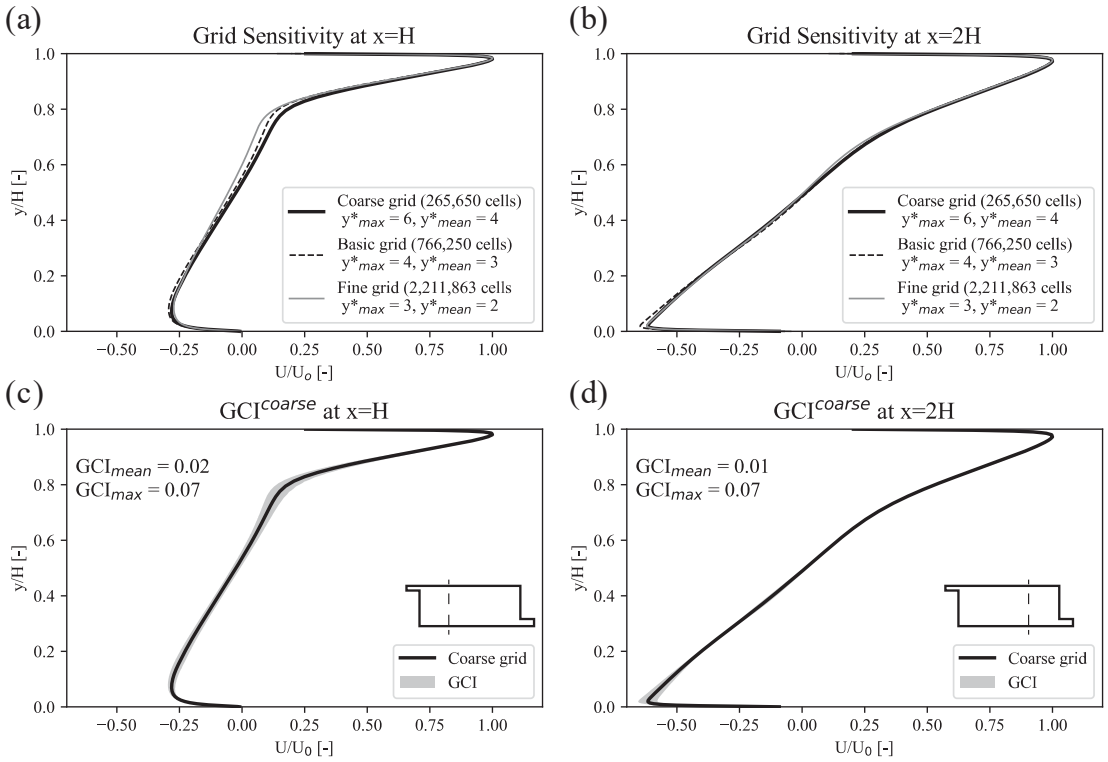

Fig. 4 –Grid-sensitivity analysis at (a) x=H, (b) x=2H. GCI plot at (c) x=H, (d) x=2H.

2.3 vCFD methodology

The vCFD simulations are performed via the steady solver in ANSYS Discovery 2021 R2. The software requires basic input in the form of boundary conditions. The solver settings cannot be adjusted and several proprietary aspects of the software remain undisclosed. Turbulence modeling is performed using the Standard $k-\epsilon$ model. Pressure and velocity are coupled via the use of a SIMPLE-like algorithm. Simulation convergence is determined automatically.

The voxel-based grid is sized according to the available video memory (VRAM). The highest fidelity setting discretizes the domain using $40.21\,mm$ voxels. The total count is equal to 1,338,095 voxels. The vCFD grid is shown in **Fig.3c**.

3. Hardware configurations

All simulations are performed on a HP Zbook Studio G5 laptop, equipped with an Intel® Core™ i7-9750H central processing unit (CPU) and 16 GB of random access memory (RAM). The CPU consists of six physical cores and six logical processors, which run at a base clock speed of 2.60 GHz. Hyperthreading is disabled to ensure efficient use of physical cores. The laptop is equipped with an NVIDIA Quadro P2000 graphical processing unit (GPU) with 4 GB video memory (VRAM). Six CFD configurations and six cCFD configurations are tested using 1-6 physical cores and one vCFD simulation is run on GPU. The computational domain is divided into n partitions, corresponding to the number of active CPU cores.

4. Ventilation design quality

While there exist multiple ways to evaluate the quality of a given design, most engineers refer to standards for quality assurance. Using the available experimental data, the draught rate DR is computed using equation (6), where $T_a = 20℃$ is the air temperature, v is the mean velocity magnitude and I is the turbulence intensity.

$$\mathrm{DR} = (34 - T_a)(v - 0.05)^{0.62} \\ (37 \cdot I \cdot v + 3.14) \qquad (6)$$

DR is then computed via vCFD, cCFD and CFD and compared to a hand calculation (EMP), based on a series of engineering assumptions. The maximum velocity in the occupied zone u_{rm} is obtained using the empirical formula stated in equation (7), where the decay constant for a plane wall jet K_p is 3.5 [14], the decay constant in the recirculation region K_{rm} is 0.7 [15] and the distance from the virtual origin of the diffuser x_0 is 3 m.

$$\mathrm{u_{rm}} = \mathrm{K_p K_{rm} u_0}\sqrt{\frac{\mathrm{h}}{\mathrm{L}+\mathrm{x_o}}} \qquad (7)$$

Given that turbulence intensity information is unavailable for vCFD and EMP, $10\% \leq I \leq 90\%$ is used to account for the range of values that may be used as input. The results are used to discuss the potential contribution of FNMs towards ventilation design, beyond that of engineering tools.

5. Results

5.1 isothermal validation study

Fig. 5a-5b show the dimensionless mean velocity profiles obtained using vCFD, cCFD and CFD, in comparison with the available experimental data. The results show that all three numerical methods capture the primary characteristics of the mixing ventilation flow, such as the high-velocity region near the ceiling and the recirculation flow in the occupied zone. **Fig. 5c-5d** compare the accuracy of the three numerical methods. No single numerical method outperforms the others across all metrics. The RMSE values for vCFD, cCFD and CFD are 0.05, 0.09 and 0.05, respectively, suggesting that the accuracy of vCFD and CFD is comparable. The FAC1.1 values for vCFD, cCFD and CFD are 0.26, 0.26 and 0.32, indicating that CFD gives the best agreement with the experimental data. The FAC1.2 values are 0.60, 0.50 and 0.68 and the FAC1.3 values are 0.62, 0.60 and 0.60, respectively. The best performing method differs per metric and, given that the relative difference in performance is small, the accuracy of vCFD, cCFD and CFD for this validation case is considered commensurate. **Fig. 5e** shows the computational time per simulation, in minutes. The results show that the fast numerical methods are two orders of magnitude faster than CFD. Moreover, the decrease in computational time obtained from parallel processing is almost linear as the number of cores is increased but exhibits stagnant behaviour after a certain number of cores. The stagnation may be attributed to a number of hardware or software related factors [16], one of which is the low cell count used for this validation case. It is concluded that fast numerical methods are significantly faster than conventional CFD and that shared-memory parallel simulation does not change the outcome in favor of using CFD for ventilation design optimization.

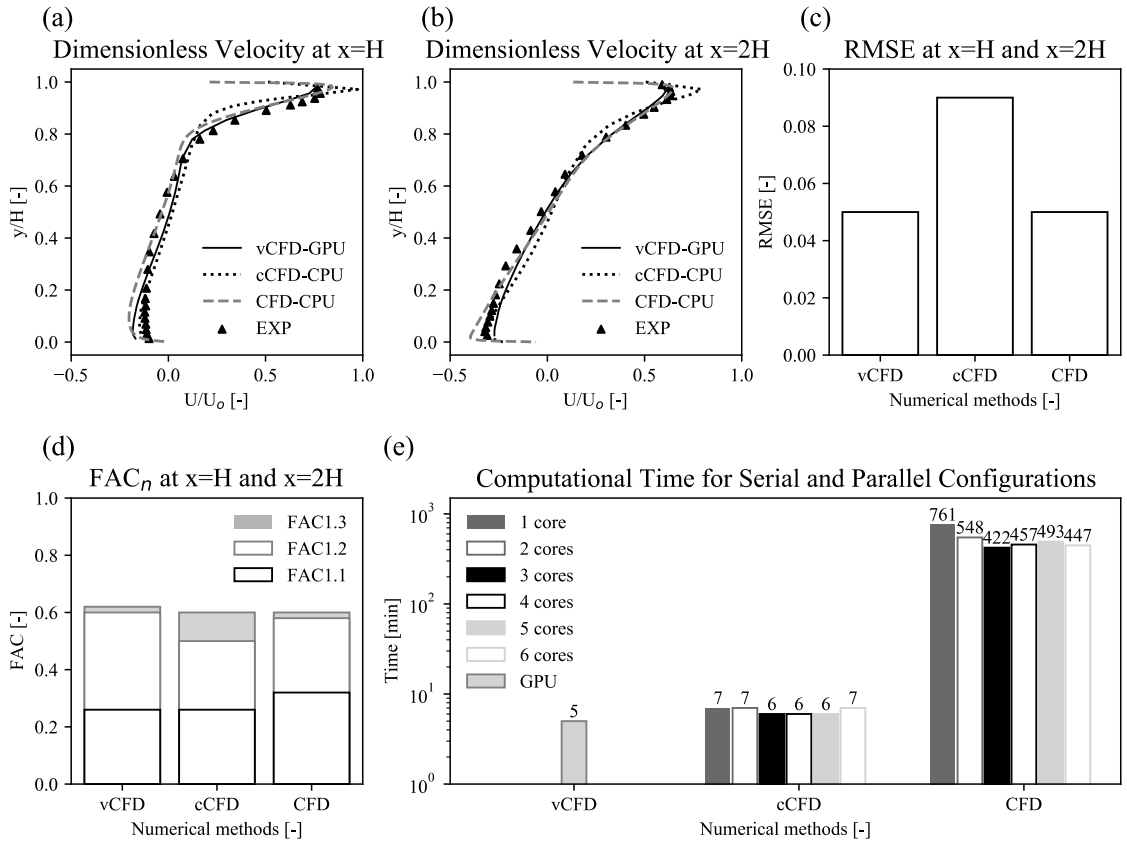

Fig. 5 – Results for vCFD, cCFD and CFD. (a)-(b) Dimensionless velocity profiles at x=H and x=2H. (c) RMSE for vCFD, cCFD and CFD. (d) FAC1.1, FAC1.2 and FAC1.3 for vCFD, cCFD and CFD. (e) Computation time for vCFD, cCFD and CFD.

5.2 ventilation design quality

Tab. 2 reports the maximum DR in the occupied zone, computed according to equation (6), as well as the maximum velocity in the occupied zone u_{rm} and the turbulence intensity I. For the CFD-based methods, the search for u_{rm} and maximum DR is conducted at z = 0.5W. For EMP, u_{rm} is computed via equation (7). The empirical model yields the lowest $u_{rm} = 0.14\ m/s$, followed by vCFD, CFD and cCFD at $0.18\ m/s$, $0.20\ m/s$ and $0.24\ m/s$, respectively. The latter three values are relatively comparable in magnitude and are located near the outlet. Meanwhile, EMP assumes that u_{rm} occurs at $x = 2H$. It is not possible to validate the accuracy of the u_{rm} calculations due to the absence of measurement data. However, the discrepancy in location suggests that EMP does not have the spatial sensitivity to predict u_{rm} and that FNMs allow for more effective optimization of local comfort parameters. The maximum DR values lie above 10% (categories II-III) for all methods. The results for cCFD and CFD are

23% and 19%, placing them in categories III and II, respectively. The results for EMP and vCFD span both categories, given the range $10\% \leq I \leq 90\%$ used for the calculation. This illustrates that, in the absence of numerical data, ventilation design quality is sensitive to user input, which can lead to uncertainty in ventilation design quality. For this validation case, such dependency can be reduced through the use of cCFD, which provides spatial information at a low computational cost.

Tab. 2 – Default criteria, according to [17], and calculated values related to the draught rate *DR* in the occupied zone.

Variable		EMP	vCFD	cCFD	CFD
u_{rm} $[m/s]$		0.14	0.18	0.24	0.20
I [%]		10-90	10-90	17	19
DR	[%]				
I	<10	-	-	-	-
II	<20	11-24[a]	14-31[a]	-	19
III	<30			23	-

[a] Note that the results are within categories II and III.

It is important to mention that each method has its advantages and disadvantages. For example, vCFD is performed using a commercially available software with a simple graphical user interface that could soften the barrier of entry for the engineering sector. However, the software is relatively new and further developments are ongoing. Meanwhile, cCFD can be performed using any CFD software, which allows the user flexibility in obtaining detailed spatial information. On the other hand, the implementation of cCFD implies a very similar level of CFD knowledge as conventional CFD, thereby increasing the level of expertise required for its implementation. In summation, it is highly unlikely that one method will maintain an advantage for every given case. A potential strategy for integrating FNMs in design practices is to approach the methods as components in a workflow or toolkit, perhaps even alongside engineering tools and conventional CFD.

6. Limitations and future research

This study presents first results in a larger research effort on FNMs as a toolkit for ventilation design. It is subject to several limitations which may be addressed via future research efforts:

- The validation case is based on a geometry that captures mixing flow characteristics but is too simple to be representative of a real design scenario.
- The absence of validation data inhibits the validation of important design criteria, such as the draught rate *DR*.
- The isothermal study does not account for significant influences such as windows, people and other heat sources, which will be included in ongoing and future studies.
- Other FNMs, such as zCFD, LBM and FFD, are not included in this study but are worth including in the future.

7. Conclusion

This study presents preliminary results in an effort to evaluate the potential of FNMs for improving ventilation design quality. An isothermal mixing ventilation case is simulated using vCFD, cCFD and conventional CFD. The results are compared to existing measurement data and are further used to evaluate the draught rate *DR* in the occupied zone. The outcomes are compared to that of an empirical calculation. This study offers a comparison between engineering tools, CFD, vCFD and cCFD, which, to the best knowledge of the authors, has not been made before. The following conclusions are made:

- Both conventional CFD and FNMs capture the principal characteristics of mixing ventilation flow.
- FNMs are two orders of magnitude faster than conventional CFD, for this case.
- For this validation case, the accuracy of vCFD and cCFD is comparable to that of CFD.
- The spatial resolution of vCFD, cCFD and CFD is better-suited to evaluate local parameters, such as u_{rm} and *DR*, compared to empirical models.
- In order to calculate *DR* using EMP and vCFD, an assumption for I is required. Dependency on user input introduces uncertainty in the ventilation design quality, as shown by the large variability in *DR*. In this case, cCFD offers a distinct advantage to vCFD.
- To extrapolate, the results suggest that the choice of numerical method is case-dependent. The authors do not encourage the pursuit of a one-size-fits-all.

8. Acknowledgement

The authors gratefully acknowledge the partnership with ANSYS. The authors acknowledge the support of the Flemish Agency for Innovation and Entrepreneurship (VLAIO) in the Flux50 project Smart Ventilation (HBC.2020.2520).

9. Data access statement

Data sharing is not applicable to this article as no datasets were generated or analyzed during the current study.

10. References

[1] Awbi, H.B. Ventilation systems: Design and performance. 2007; Chapter 2: 62-104.

[2] Morsli S., Ramenah H., El Ganaoui M., and Bennacer R. Effect of aligned and misaligned

ventilation openings affecting energy demand and air quality in buildings. EPJ Applied Physics. 2018; 83(1).

[3] Staveckis, A., Borodinecs, A. Impact of impinging jet ventilation on thermal comfort and indoor air quality in office buildings. Energy and Buildings. 2021; 235(5).

[4] Nielsen P.V. Strømningsforhold i luftkonditionerede lokaler (English translation: Flow in Air Conditioned Rooms). Phd Thesis. Technical University of Denmark. 1974.

[5] Morozova N., Trias F.X., Capdevila R., Pérez-Segarra C.D., Oliva A. On the feasibility of affordable high-fidelity CFD simulations for indoor environment design and control. Building and Environment. 2020; 184(May).

[6] Hosain M.L., Fdhila R.B. Literature Review of Accelerated CFD Simulation Methods towards Online Application. Energy Procedia. 2015; 75: 3307–3314.

[7] Wang H., Zhai Z. Application of coarse-grid computational fluid dynamics on indoor environment modeling: Optimizing the trade-off between grid resolution and simulation accuracy. HVAC and R Research. 2012; 18(5), 915–933.

[8] Papp B., Kristóf G., Gromke C. Application and assessment of a GPU-based LES method for predicting dynamic wind loads on buildings. Journal of Wind Engineering and Industrial Aerodynamics. 2021; 217.

[9] Chen Q., Xu W. A zero-equation turbulence model for indoor airflow simulation. Energy and Buildings. 1998; 28(2): 137–144.

[10] Khan M.A.I., Delbosc N., Noakes C.J., Summers J. Real-time flow simulation of indoor environments using lattice Boltzmann method. Building Simulation. 2015; 8(4): 405–414.

[11] Liu W., Van Hooff T., An Y., Hu S., Chen C.W. Modeling transient particle transport in transient indoor airflow by fast fluid dynamics with the Markov chain method. Building and Environment. 2020; 186(September).

[12] ANSYS Inc. Discovery 2021 R2. January 2021.

[13] Nielsen P.V., Rong L., Olmedo I. The IEA Annex 20 Two-Dimensional Benchmark Test for CFD Predictions. 2010.

[14] Nielsen P.V. Lecture slides on Mixing Ventilation. University of Aalborg. Accessed on 14 Dec 2021.

[15] Nielsen P.V. Numerical Prediction of Air Distribution in Rooms – Status and Potentials. University of Aalborg. 1988.

[16] ANSYS Inc. Parallel Processing Guide. 2021.

[17] NEN-EN 16798-1: 2019 - Energy performance of buildings - Ventilation for buildings - Part 1: Indoor environmental input parameters for design and assessment of energy performance of buildings addressing indoor air quality, thermal environment, lighting and acoustics - Module M1-6. 2019.